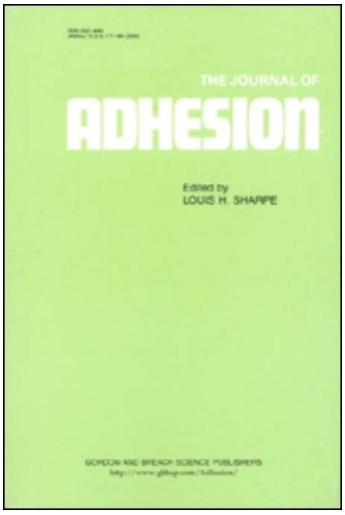

The Journal of Adhesion
Publication details, including instructions for authors and subscription information:
http://www.informaworld.com/smpp/title~content=t713453635

Surface Mechanical Properties of the Spore Adhesive of the Green Alga *Ulva*

Gilbert C. Walker[a]; Yujie Sun[b]; Senli Guo[b]; John A. Finlay[c]; Maureen E. Callow[c]; James A. Callow[c]
[a] Department of Chemistry, University of Toronto, Toronto, Ontario, Canada [b] Department of Chemistry, University of Pittsburgh, Pittsburgh, Pennsylvania, USA [c] School of Biosciences, University of Birmingham, Birmingham, UK

To cite this Article Walker, Gilbert C. , Sun, Yujie , Guo, Senli , Finlay, John A. , Callow, Maureen E. and Callow, James A.(2005) 'Surface Mechanical Properties of the Spore Adhesive of the Green Alga *Ulva*', The Journal of Adhesion, 81: 10, 1101 — 1118
To link to this Article: DOI: 10.1080/00218460500310846
URL: http://dx.doi.org/10.1080/00218460500310846

The Journal of Adhesion, 81:1101–1118, 2005

ISSN: 0021-8464 print/1545-5823 online
DOI: 10.1080/00218460500310846

Taylor & Francis
Taylor & Francis Group

Surface Mechanical Properties of the Spore Adhesive of the Green Alga *Ulva*

Gilbert C. Walker
Department of Chemistry, University of Toronto, Toronto, Ontario, Canada

Yujie Sun
Senli Guo
Department of Chemistry, University of Pittsburgh, Pittsburgh, Pennsylvania, USA

John A. Finlay
Maureen E. Callow
James A. Callow
School of Biosciences, University of Birmingham, Birmingham, UK

The mechanical properties of the adhesive produced by spores of the green, marine, fouling alga Ulva linza are reported. Atomic force microscopy studies were performed and nanoindentation data were analyzed using a model for an asymmetric indenter. Freshly secreted adhesive is characterized by multiple layers. We found that the modulus of the outer $\sim$*600-nm thick layer was about* 0.2 ± 0.1 *MPa, whereas the modulus of the inner layer was about* 3 ± 1 *MPa. Older adhesive showed the formation of a "crust" of harder material with a yield strength of* $\sim$*20 MPa at a loading rate of* 2.5×10^{-6} $N \cdot s^{-1}$. *Mechanical properties under tension are also described, and extension profiles that showed either constant or nonlinear force changes with tip-sample separation were observed. Models for both kinds of behavior are described. The work of adhesion between poly-dimethylsiloxane (PDMS)-coated AFM tips and the adhesive was determined to be less than* $1.5\ mJ \cdot m^{-2}$.

Keywords: *Ulva*; Marine alga; Atomic force microscope; PDMS; Bioadhesive

Received 3 February 2005; in final form 26 July 2005.

One of a collection of papers honoring Manoj K. Chaudhury, the February 2005 recipient of The Adhesion Society Award for Excellence in Adhesion Science, sponsored by 3M.

Address correspondence to Gilbert C. Walker, Department of Chemistry, University of Toronto, Toronto, ON, M5S 3H6, Canada. E-mail: gwalker@chem.utoronto.ca

INTRODUCTION

Marine biofouling is characterized by "soft" and "hard" fouling organisms, often represented by algae in the former case and tubeworms and barnacles in the latter. These fouling organisms increase the hydrodynamic drag on marine vessels [1]. Although biocides have represented the favored practical method to inhibit the growth of fouling organisms, recent developments in environmental regulation have forced work toward the development of materials and coatings that control marine growth without biocides. Some of these materials function by allowing easy release of the fouler, for example by way of using flexible, "foul-release" silicone elastomer [2–4]. Nonetheless, knowledge of the basic possible mechanisms of the release of marine organisms from surfaces is limited. For example, the chemical composition of the adhesives of tubeworms, barnacles, and algae is only poorly known. Knowledge of the mechanical properties [2, 5] and surface energies of the marine adhesives and their failure mechanisms is also limited but would be a useful input into the design of antifouling surfaces.

Green algae of the genus *Ulva* (formerly *Enteromorpha* [6]) are common, green macroalgae found throughout the world in the upper intertidal zone of seashores and as a fouling organisms on a variety of man-made structures including ships' hulls [7]. Dispersal is achieved mainly through asexual zoospores; quadriflagellate, pear-shaped cells, 5–7 μm in length. Colonization of substrata involves the transition from a free-swimming spore to an adhered nonmotile spore [8]; adhesion is achieved *via* the exocytotic secretion of an adhesive glycoprotein, which is present in spores in highly condensed form within vesicles [9]. On release initially fluid adhesive swells rapidly through the adsorption of water to form a gel-like pad on the surface [10]. It then starts to undergo cross-linking with a corresponding increase in adhesion strength [11].

Atomic force microscopy (AFM) has been used previously to examine the adhesive properties of the secreted spore adhesive of *Ulva* and how these change with time after release [5]. The present article aims to extend the analysis of secreted spore adhesive using AFM to explore the surface mechanical and viscoelastic properties in more detail. We have used cantilevers functionalized in various ways to explore the influence of surface chemistry on tip–sample interactions. We also consider the critical stresses that lead to cohesive failure of the cured adhesive.

METHODS

Plant Material

Fertile plants of *Ulva linza* were collected from Wembury Beach, England (50°18′ N; 4°02′ W). Zoospores were released and prepared for experiments as described previously [8].

Settlement of *Ulva* Zoospores for AFM Measurements

Zoospores were settled in individual 35-mm diameter polystyrene (PS) Petri dishes containing 10 ml of zoospore suspension, in the dark at ~20°C, as described previously [5]. After a settling period of 5 min, unsettled spores were removed by rinsing with filter-sterilized artificial seawater (Instant Ocean) and the dishes placed under the microscope, with first imaging typically occurring within 10–15 min after settlement. To take measurements from adhesive pads (which cannot be seen in the optical microscope) the methods described by Callow *et al*. [5] were used. Settled spores were located with the optical objective and manually brought to a position adjacent to the cantilever tip. Force curves were then sampled for the polystyrene substrate as the cantilever was slowly advanced toward the attached spore. Contact between the cantilever and the adhesive pad was readily recognized by a distinct change in the force plots.

Atomic Force Microscopy

Height, adhesion, and friction measurements were performed at ambient temperature (20°C) with a Digital Instruments (Santa Barbara, CA, USA) Dimension 3100 scanning force microscope equipped for operation under fluids. Methyl- and carboxylic acid–coated probe tips were purchased from BioForce Laboratory (Ames, Iowa, USA). Tips coated with a monolayer of grafted poly-dimethylsiloxane (PDMS) were made as described in following paragraphs. These tips were made less than 1 week before use and were stored under an argon atmosphere until 1–2 days before use.

Images of the tip were obtained on the silicon-tip grating (grating-tip radius is specified <10 nm by the manufacturer, NT-MDT Co., Moscow, Russia) and inspected to extract the cantilever-tip radius. Tip radius was determined to be *ca*. 50 nm. Tip force constants were either used as given by the manufacturer or measured by the Hutter [12] or Sader [13] methods, as indicated where relevant.

AFM Data Analysis

Software provided with the Nanoscope IIIa microscope (Digital Instruments, Santa Barbara, CA, USA) was used to collect height, lateral force, and force *vs* distance curves (often called force plots). For each experiment we collected force *vs* distance curves as a function of the tip position on the surface. The data were subsequently analyzed using custom software. Force curves were collected for scanner approach and retract. Custom software written in MATLAB (Natick, MA, USA) was used to extract the modulus from the experimental indentation measurements. The viscoelastic properties were evaluated by collecting data at different velocities of cantilever base motion relative to the substrate.

Preparation of PDMS Monolayers

PDMS grafting was done on both silicon cantilevers for AFM studies and glass slides for whole-cell hydrodynamic adhesion studies. The PDMS used was 2000–3000 MW, prepared in monolayers according to the literature [14]. The sessile contact angle of nanopure water on PDMS-grafted glass was $103 \pm 1^{\circ}$; on PDMS-grafted silicon, it was $100 \pm 1^{\circ}$.

Contact-Angle Measurement

A homemade apparatus was used to do the contact-angle measurement. Measurements were made using static droplets of millipure water. Contact angles represent the mean from four measurements.

Measurement of Whole Spore Adhesion Strength

Zoospores were released and prepared for attachment experiments as described in Callow *et al*. [18]. Ten-ml aliquots (1.5×10^6 spore ml^{-1}) were pipetted into individual compartment of Quadriperm polystyrene culture dishes (Fisher, Pittsburgh, PA, USA), each containing either a control glass microscope slide (acid-washed in a 50% methanol/50% concentrated hydrochloric acid mixture, followed by 100% concentrated hydrochloric acid (2 h in each) or a glass slide coated with a PDMS monolayer. Six replicate dishes were incubated in the dark for 1 h before the slides were washed by passing backward and forward 10 times through a beaker of seawater to remove unattached spores. Three replicate slides from each treatment were fixed in 2.5% glutaraldehyde in seawater and processed as described in Callow *et al*. [18].

The remaining three replicates were placed in a flow apparatus [15] that had been modified by fitting a higher-capacity pump as described in Finlay *et al*. [11]. Slides were exposed to a fully developed turbulent flow for 5 min at 55-pa wall shear stress. After fixing slides in 2% glutaraldehyde, adhered spores were visualized by autofluorescence of chlorophyll and quantified by image analysis as described in Callow *et al*. [16]. Thirty counts were taken at 1-mm intervals along the middle of the long axis of each of the three replicate slides. The mean number of spores remaining attached to the surface after exposure to turbulent flow was compared with the mean number before the slides were subjected to flow. Data are presented in terms of spore density on the two types of surface and the percentage of spore removal, $\pm 95\%$ confidence limits calculated from arcsine-transformed data.

RESULTS AND DISCUSSION

In the AFM experiment, the curve illustrating forces on the cantilever upon approach to the surface provides information on surface modulus, plasticity, and viscosity [17]. In analyzing approach data, we ignore plastic and viscous effects. The hysteresis between approaching and retracting curves provides information on energy dissipation and the viscoelastic properties of the sample. The rupture energy, which is the area between approaching and retracting curves upon detachment, provides information regarding the tip–sample interfacial energy. Analysis of the tethering forces in retracting curves after the contacting hemisphere of the tip has ruptured from the surface provides information on the unraveling of polymer blobs and entropic springs of polymer chains. These phenomena were observed and are reported.

Figure 1 illustrates the appearance of a settled spore on a surface, as visualized by environmental scanning electron microscopy (ESEM) [10]. The prominent settled spore, which is approximately 5 μm in diameter, is surrounded by an annular pad of secreted adhesive material; the whole object is approximately 20 μm in diameter. In view of the small size of the object and the transparency of the adhesive pad under the AFM optical objective, location of the cantilever tip onto the adhesive pad to obtain force plots involved a procedure whereby force curves were monitored as the tip was gradually moved toward the adhesive pad. The transition between the polystyrene surface and the adhesive pad could be readily recognized. However, the need for this procedure inevitably prolonged the time before measurements could be made so that, in practice, it was not possible to sample adhesive properties earlier than 15 min after initial settlement.

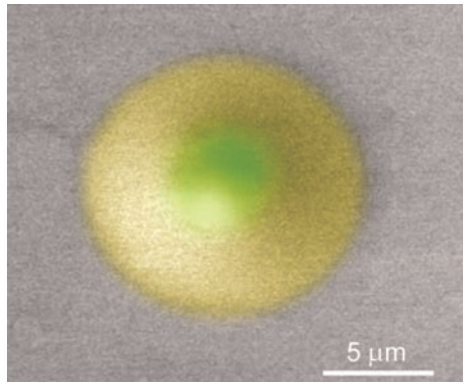

FIGURE 1 False image of a settled spore obtained by environmental scanning electron microscopy, illustrating the corona of secreted adhesive surrounding the spore body. The image is $30 \times 30\,\mu m^2$.

Indentation Force Reveals Multilayer Structure of Spore Adhesive

The elastic modulus of a material determines how much force must be applied to stretch it by a given length or how deeply a probe will indent a material when a force is applied [18]. Fresh spore adhesive (*i.e.*, approximately 15 to 20 min after release) was indented by the AFM tip to measure the modulus, as illustrated in Figure 2. The figure shows two characteristic regions in the force-indentation curve. We use Sneddon mechanics to model the elastic deformation [19]. We calculate sample indentation by considering a rigid axisymmetric tip under an applied load [20–33]. The layer and the substrate deformations are considered to be purely elastic; in this indentation analysis we do not consider viscoelastic and plastic deformation effects. These measurements are interpreted using a model that includes a paraboloidal or conical tip that elastically indents a half-space sample. The elastic modulus of a semi-infinite sample can be estimated using load-indentation dependencies as follows:

$$F = \frac{2E\tan(\alpha)}{\pi(1-\sigma^2)}\delta^2 \tag{1a}$$

$$F = \frac{4E\sqrt{R}}{3(1-\sigma^2)}\delta^{(3/2)} \tag{1b}$$

Equations (1a) and (1b) correspond to conical and paraboloidal shapes of revolution, respectively. Here F is load; δ, indentation; R, tip radius

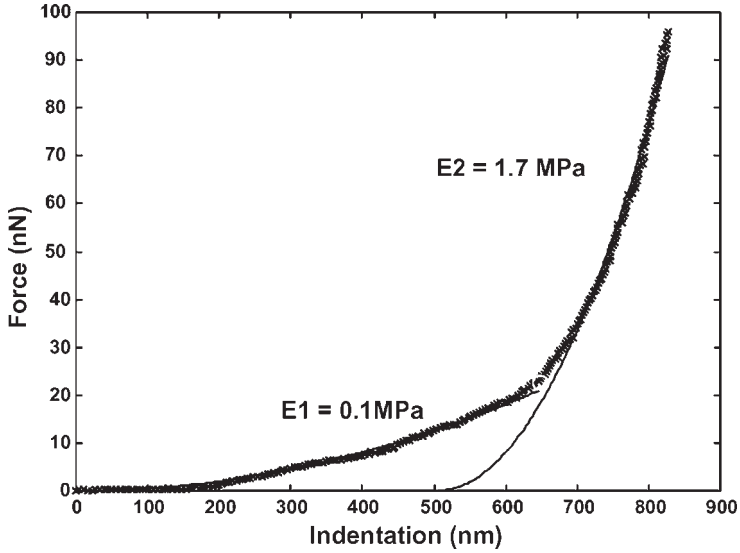

FIGURE 2 Force *versus* indentation plot for freshly released spore adhesive. The crosses are data, and they are fit by two lines representing two consecutive layers of elastic material being indented by a conical probe according to the Sneddon model. E1 and E2 are the two characteristic elastic moduli.

of curvature; α, tip semivertical angle; E, Young's modulus; and σ, Poisson's ratio. Using the Sneddon model for two noninteracting layers, we found that the modulus of the outer $\sim$600-nm thick layer was about 0.2 ± 0.1 MPa, and the modulus of the inner layer was about 3 ± 1 MPa. The obtained modulus for the outer layer of fresh adhesive is comparable with previous results by Callow *et al*. [5], although previous studies did not note the multilayer aspect of fresh adhesive. Multilayer adhesive structures were also observed in the studies of Sun *et al*. of barnacle baseplates that had been forced from PDMS elastomer substrates [2]. Adhesive pads older than about an hour following settlement showed displacements in the approach curve that would be consistent with the formation of a harder crust (Figure 3), indicative of a more rapid curing of the surface layer with time. It was not possible to use the Sneddon model on such data to compute modulus values comparable with those for freshly secreted adhesive. Conversely, it is possible to roughly estimate the yield strength of the crust by considering the ratio of the breakthrough force and approximating the contact area as a hemisphere of the tip radius, which was $\sim$20 MPa at a loading rate of 2.5×10^{-6} N $\cdot$ s^{-1}.

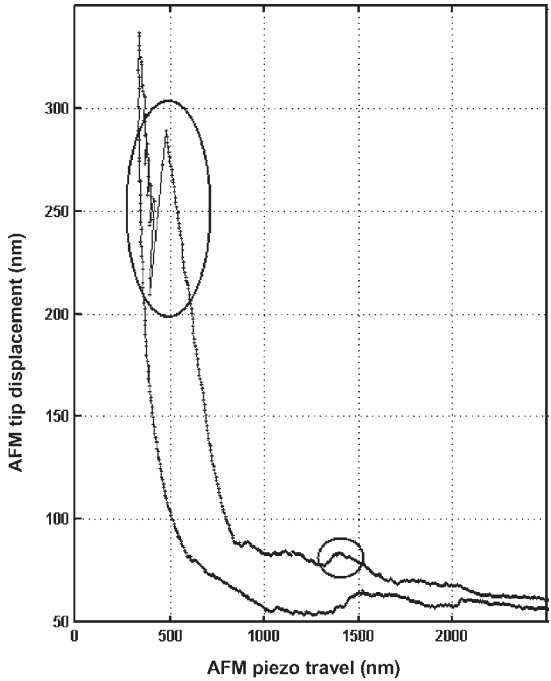

FIGURE 3 Tip displacement *versus* piezo displacement, showing sudden transitions where the tip breaks through the crust of 1-h-old spore adhesive (transitions can be seen within the ellipses). The upper line shows dip displacement upon approach, and the lower line provides the retract data. The characteristic position of the feature seen within the lower ellipse moved to higher force at greater loading rates, which precludes its assignment as optical interference.

Adhesive under Tension Reveals Polymer Blob Unraveling Dynamics

A polymeric adhesive under tensile stress can undergo structural changes that balance the stretching energy of the molecules with the interfacial energy of the necks or tendrils of adhesive that appear as the adhesive is strongly distorted [34]. In this work, the forces acting upon withdrawing AFM tips in contact with spore adhesive were measured. In the previous AFM study of spore adhesive [5], the emphasis was on determining the strength of adhesion whereas the present study aimed to characterize other viscoelastic properties. In the present study, although force plots with large adhesions were observed, force plots of the kind seen in Figure 4 were also common,

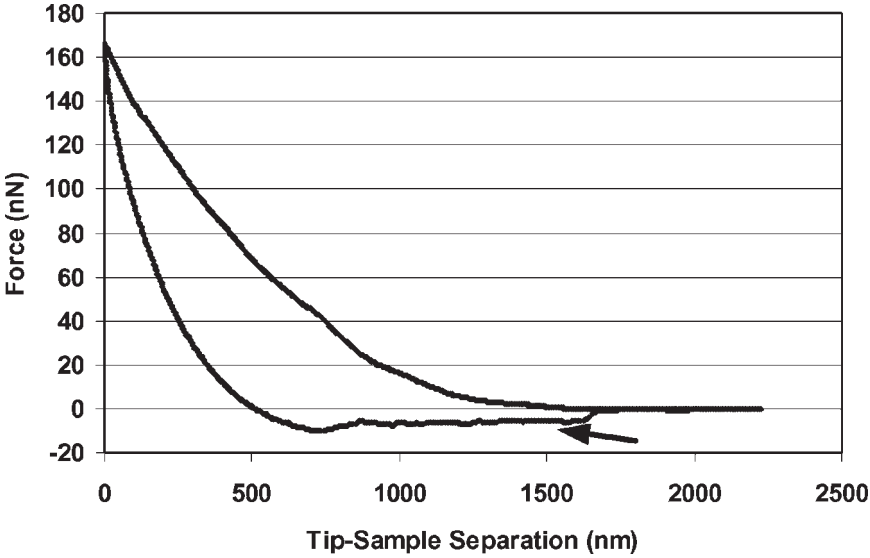

FIGURE 4 Forces acting on a carboxylate-terminated alkane thiol grafted AFM tip as it moves toward and away from adhesive of spores 15 min after settlement. The upper curve shows the forces upon approach, and the lower curve shows the forces upon tip retraction. The arrow indicates an extended region where the force attracting the tip to the surface is nearly constant upon retraction.

and these were observed with both $-CH_3$- and $-COOH$-terminated AFM tips. In such plots the restoring force upon tip withdrawal is largely constant and nonzero over an extended region of tip withdrawal (see the region between 700 and 1700 nm). This constant force arises out of a balance of material–liquid interaction energy and material entropy, yielding mechanics that we describe next.

Because of the solvophobic interactions, the chains on the spore adhesive surface aggregate into "surface blobs" [35, 36]. Such blobs consist of a droplet-like core of collapsed polymers and "legs" that anchor the core to the rest of the surface. Because of the interaction between the polymer and AFM tip, the core can partially wet the tip and form a spherical cap at contact. At larger tip-sample separation, polymer chains aggregate into a cylindrical strand. The free energy per chain in the strand involves losses due to the elastic stretching of the chains, and the surface free energy associated with the surface of the cylinder. By minimizing the free energy with respect to the number of monomers per chain in the cylinder, n, at a fixed value of

the cylinder height, one could obtain the equilibrium value of n. The cylinder radius does not depend on the height of the cylinder but remains constant in value. As the tip-sample separation is increased, the cylinder height also increases. An increase in cylinder height necessitates an increase in the number of monomers per chain in the cylindrical strand. The additional monomers are extracted from the micellar core, the reservoir of available units, and are localized in the cylindrical strand. These additional units maintain the radius of the strand and effectively mediate the effects of the applied force. Put concisely, the unraveling of the blob's core gives rise to a profile where the restoring force does not depend on tip-sample separation. In principle, the magnitude of the constant force can be obtained from a knowledge of the energies of the participating surfaces, but adequately accurate estimates of these energies could not be obtained in this work, and the observation that both $-CH_3$- and $-COOH$-coated tips are involved in such force plots may indicate that the adhesive surface does not have a spatially uniform surface energy.

If the polymer had a favorable interaction with the solvent, an entropic, increasing response due to chain ordering would primarily be seen and not the flat response seen here. Hence, it may be concluded that parts of the polymer are self-associating in aqueous solution and most likely lying in spherical blobs that can be distorted by the force of a withdrawing tip. We found this kind of force profile was more common for adhesive that was recently released; hence, we concluded that fresh adhesive is more hydrophobic than aged adhesive. Additionally, the adhesive was probably not extensively cross-linked because such cross-linking would inhibit the molecular flow associated with minimizing the adhesive surface area as the blob is distorted.

Adhesive under Tension Reveals Nonlinear Restoring Force due to Elastic Response

In other force plots, the AFM tip (both $-CH_3$ and $-COOH$ terminated), once it had contacted the adhesive, encountered regions from which it was difficult to break free (see for example Figure 5, where the force–distance profile is shown). The adhesive remained stuck to the AFM tip and exhibited a nonlinear elastic response. We have applied a simple model for this elasticity, called the worm-like chain (WLC) model. This is one of several well-known models for single-chain mechanics, which evaluate the predominant role of entropy in determining chain conformation and hence elasticity [37].

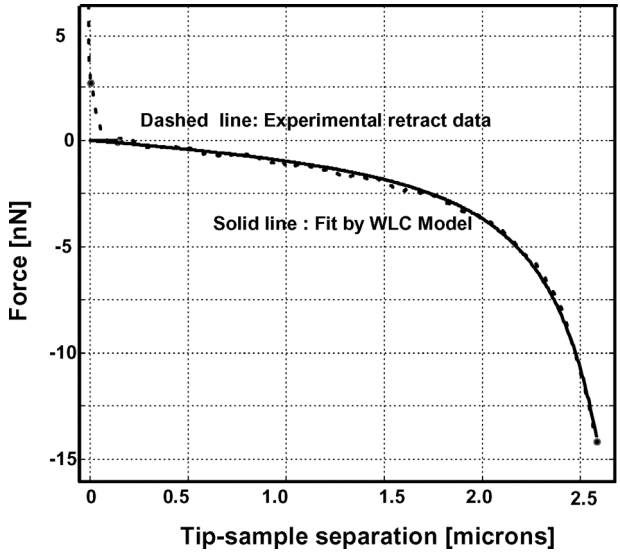

FIGURE 5 Pulling the adhesive away from the surface using a methyl-terminated alkane thiol grafted AFM tip. The data exhibit a nonlinear restoring force upon extension. Worm-like chain (WLC) model is fit to the experimental data. The persistence length obtained from fit is 100× smaller than for a typical single glycoprotein chain, thus, indicating ∼100 chains in a rope are being stretched in under tension.

The WLC model, which describes the elastic restoring force of a polymer chain caused by the reduction in available configurations as the end-to-end distance is increased, has been used before for characterizing AFM tip-induced chain extensions. The WLC model predicts a force–distance dependence described by Equation (2):

$$F = (k_b \cdot T/A) \cdot [0.25 \cdot (1 - R)^{-2} - 0.25 + R] \quad (2)$$

Here F is the tension between two points (nN), k_b and T are the Boltzmann constant (J/K) and temperature (K), respectively; A is the persistence length (nm); and R is the unitless extension ratio. The extension ratio is the fraction of the polymer contour length that the chain is extended. If points A and B are separated by distance x, the extension ratio is x divided by the contour length of the chain between points A and B. For the extension of parallel chains, under the assumption that the chains are noninteracting, the fitted persistence length is proportionately reduced by the number of chains in parallel; *i.e.*, $A_{\text{fitted}} = n^{-1} * A_{\text{singlechain}}$. The persistence length obtained

in the fit shown in the Figure 5 is ~ 0.003 nm, indicating about 100 chains participate in the rope [38].

Elastic-stretching and blob-distortion phenomena were not uniquely associated with measurements made using a given tip type. Furthermore, tips became fouled with adhesive after repeated contact with the surface, although we changed tips upon observing such phenomena. Concerns regarding tip fouling precluded our efforts to evaluate tip–polymer interaction energies for $-CH_3$- and $-COOH$-terminated tips.

Viscoelastic Behavior of the Adhesive

We found a hysteresis between the loading and unloading force curves when the spore adhesive was being stretched. The hysteresis can be caused by viscoelastic effects or by bond breaking/making effects. Viscoelastic materials are those for which the relationship between stress and strain depends on time. Some phenomena in viscoelastic materials are (i) if the stress is held constant, the strain increases with time (creep); (ii) if the strain is held constant, the stress decreases with time (relaxation); (iii) the effective stiffness depends on the rate of application of the load; and (iv) if cyclic loading is applied, hysteresis (a phase lag) occurs, leading to a dissipation of mechanical energy [39]. The loading-rate dependence of the force hysteresis was measured for spore adhesive (see Figure 6), and the profiles indicate that viscoelastic effects are responsible for the hysteresis. In Figure 6, the force gap chosen is the value where the hysteresis is greatest, and we make the simplifying assumption that one molecular rate process determines the material relaxation time.

The slope of less than 1 seen in Figure 6A implies stress "thinning" or pseudoplastic behavior, probably caused by molecular entanglements in the spore adhesive bridging the tip and surface. A schematic of the molecular process is illustrated in Figure 6B. The implication of this finding is that the force required to remove spores depends on how fast the force is applied. An important outstanding question is whether the mechanism of release of this "soft fouler" is due predominantly to cohesive or adhesive failure. The ESEM studies by Callow *et al*. [10] revealed "footprints" representative of both types of failure but more quantitative studies are needed to resolve this question.

Work of Adhesion between Tips with PDMS Monolayer Coatings and Spore Adhesive

Most fouling organisms attach weakly to low surface energy materials including those based on PDMS (*e.g*., Kavanagh *et al*. [40]; Sun *et al*.

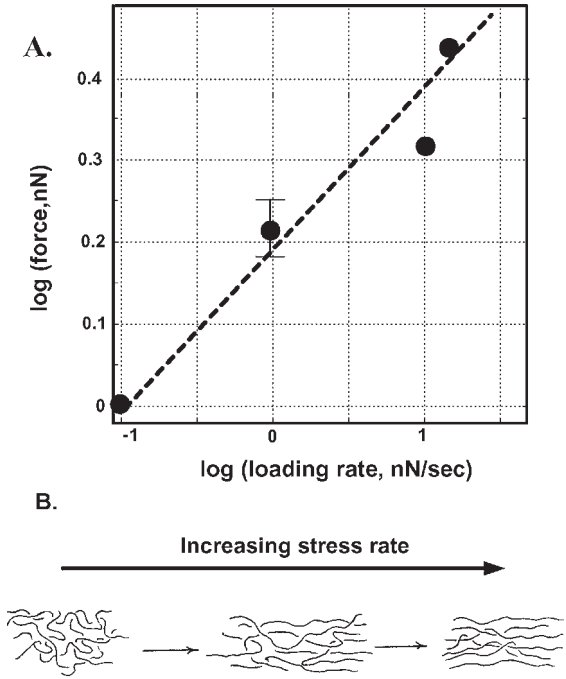

FIGURE 6 A) The plot of log-strain difference *versus* log of loading rate is linear, indicating activated dynamics and viscoelasticity. (Strain difference or force gap between loading and unloading curves was measured at a fixed value of WLC chain extension ratio [$R \approx 0.6$]). B) Effect of repeated stress on material at increasing rate. Normally, the distribution of chain conformations is randomly entangled. Under stress, those chains become ordered, and it takes time for them to randomize, which is detected by the increasing strain difference.

[2]). It was of particular interest, therefore, to explore whether weak attachment to PDMS in *Ulva* is reflected in the intrinsic adhesive properties of the spore adhesive. For this purpose, we determined the work of adhesion between AFM tips coated with a monolayer of grafted PDMS and the spore adhesive pad. However, before this it was necessary to demonstrate enhanced release of attached spores from PDMS as a monolayer. Figure 7 shows that significantly more spores settled on the PDMS monolayer than on glass (which is consistent with previous observations that spores prefer to settle on hydrophobic surfaces [41]. The strength of attachment of spores on PDMS was less than on glass because under turbulent flow conditions there

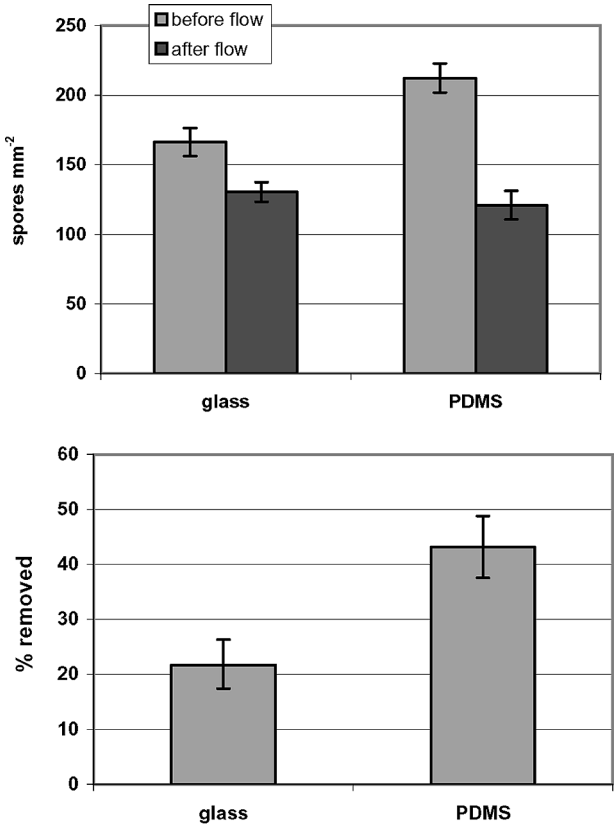

FIGURE 7 Top: Spore settlement density before and after exposure to turbulent flow. Each point is the mean of 90 counts, 30 from each of three replicates. Bars show 95% confidence limits. Bottom: Percentage removal of spores after exposure to a wall shear stress of 55 Pa. Each point is the mean of 90 counts, 30 from each of three replicates. Bars show 95% confidence limits from arcsine-transformed data.

was greater removal of attached spores from the PDMS monolayer compared with the acid-washed glass control.

The rupture forces of a PDMS-monolayer-coated tip interacting with a freshly settled spore (*ca*. 15 min after settlement) are shown in Figure 8. It can be seen that the rupture force of the PDMS-coated tip from the spore is much smaller (more than 50 times as small) than the corresponding force on the polystyrene substrate. This information can be used to estimate the work of adhesion between PDMS and the spore adhesive. The work of adhesion between PDMS

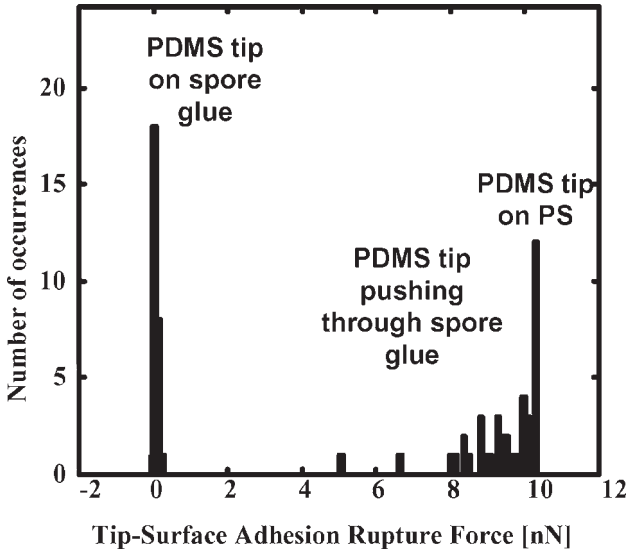

FIGURE 8 Rupture force for a PDMS-grafted AFM tip from polystyrene (PS) is more than 50 times greater than for PDMS from spore adhesive. Hence, using JKR theory, the measured work of adhesion is more than 50 times less that of the PDMS–PS adhesion work in water or the PDMS-adhesive work of adhesion in water is less than $1.5\,\mathrm{mJ}\cdot\mathrm{m}^{-2}$.

and polystyrene is approximately 50–75 $\mathrm{mJ}\cdot\mathrm{m}^{-2}$ in water [42]. JKR theory indicates that the rupture force is proportional to the work of adhesion [43]. Assuming this applies, the work of adhesion between the fresh spore adhesive and the PDMS tip is less than $1.5\,\mathrm{mJ}\cdot\mathrm{m}^{-2}$. Unlike the simple case in the PDMS tip to PS surface interaction, the spore glue is soft and viscous, and when a tip pulls the glue, there are several concerns worth mentioning. The contact radius in this case is hard to know. The equilibrium assumptions of JKR may not be valid. The maximum unloading force may not be the rupture force. The low stiffness of spore glue may result in a low apparent rupture force. Taking all of these effects into consideration, we believe $1.5\,\mathrm{mJ}\cdot\mathrm{m}^{-2}$ is a likely upper bound to the work of adhesion between the fresh spore adhesive and the PDMS tip. By way of comparison, we note that *Pseudomonas putida* bacteria under water [44] have been observed to adhere to a OH-terminated self-assembled monolayer (SAM) with a work of adhesion equal to $1.44\,\mathrm{mJ}\cdot\mathrm{m}^{-2}$, and to a methyl-terminated SAM with a work of adhesion of $7.66\,\mathrm{mJ}\cdot\mathrm{m}^{-2}$.

SUMMARY

We have examined the elastic and viscoelastic properties of *Ulva* adhesive. Both indentation and stretching studies were undertaken. Fresh adhesive was found to be multilayered, and cured adhesive formed an additional crust, presumably involving a water-triggered cross-linking reaction. Evidence of mechanical entanglements was found from a velocity-dependent adhesive-stretching experiment. An upper bound to the work of adhesion between fresh spore adhesive and the PDMS-coated tip was determined.

Our findings of multilayer structure of a natural adhesive are not without precedent. For example, multilayer structures were found in the basal plates of barnacles adhered to silicone substrates [2]. An interesting question that is largely unanswered is the effect that this structure has on the strength of the organismal adhesion. Interface between layers often serve as the regions where cracks initiate during adhesive failure [39], although we have no significant data on this point for the alga. Conversely, multicomponent glues can be more adaptive to substrates of different surface energies, which improves at least the probability of an initial adhesion.

The stretching mechanics of the adhesive are quite consistent with expectations from man-made adhesive [37], and have also been identified for other natural adhesive [45]. Plasticity is an automatic consequence of the effective cross-linking induced when long polymer chains entangle, which leads to greater cohesive strength of the adhesive. The biological advantage of the stretching hysteresis is unclear, and an important unanswered question regards the timescales of the natural detaching forces experienced by the alga.

ACKNOWLEDGMENTS

The authors acknowledge support from the Office of Naval Research (Awards N00014-02-10521 to J. A. C. and M. E. C. award and N00014-02-1-0327 to G. C. W.).

REFERENCES

[1] Townsin, R. L., *Biofouling* **19** (supplement), 9–15 (2003).
[2] Sun, Y., Guo, S., Walker, G. C., Kavanagh, C. J., and Swain, G. W., *Biofouling* **20**, 279–289 (2004).
[3] Berglin, M. and Gatenholm, P., *J. Adhes. Sci. Technol.* **13**, 713–727 (1999).
[4] Chen, C., Wang, J., and Chen, Z., *Langmuir* **20**, 10186–10193 (2004).
[5] Callow, J. A., Crawford, S. A., Higgins, M. J., Mulvaney, P., and Wetherbee, R., *Planta* **211**, 641–647 (2000).

[6] Hayden, H. S., Blomster, J., Maggs, C. A., Silva, P. C., Stanhope, M. J., and Walland, R. J., *J. Phycol*. **38**, 277–294 (2003).
[7] Callow, M. E., *Biodeterioration Abstracts* **10**, 411–421 (1996).
[8] Callow, M. E., Callow, J. A., Pickett-Heaps, J. D., and Wetherbee, R., *J. Phycology* **33**, 938–947 (1997).
[9] Stanley, M. S., Callow, M. E., and Callow, J. A., *Planta* **210**, 61–71 (1999).
[10] Callow, J. A., Osborne, M. P., Callow, M. E., Baker, F., and Donald, A. M., *Colloids Surf. B* **27**, 315–521 (2003).
[11] Finlay, J. A., Callow, M. E., Schultz, M. P., Swain, G. W., and Callow, J. A., *Biofouling* **18**, 251–256 (2002).
[12] Hutter, J. L. and Bechhoefer, J., *Rev. Sci. Instrum*. **64**, 1868–1873 (1993).
[13] Sader, J. E., Chon, J. W. M., and Mulvaney, P., *Rev. Sci. Instrum*. **70**, 3967–3969 (1999).
[14] Al-Mawaali, S., Bemis, J., Akhremitchev, B. B., Janesko, B., and Walker, G. C., *J. Phys. Chem. B* **105**, 3965–3971 (2001).
[15] Schultz, M. P., Finlay, J. A., Callow, M. E., and Callow, J. A., *Biofouling* **15**, 243–251 (2000).
[16] Callow, M. E., Jennings, A. R., Brennan, A. B., Seegert, C. E., Gibson, A., Wilson, L., Feinberg, A., Baney, R., and Callow, J. A., *Biofouling* **18**, 237–245 (2002).
[17] Dufrene, Y. F., *J. Bacteriol*. **184**, 5205–5213 (2002).
[18] Shull, K. R., *Mater. Sci. Eng*. **36**, 1–67 (2002).
[19] Sneddon, I. N., *Int. J. Engng. Sci*. **3**, 47–57 (1965).
[20] Heuberger, M., Dietler, G., and Schlapbach, L., *Nanotechnology* **6**, 12–23 (1995).
[21] Tao, N. J., Lindsay, S. M., and Lees, S., *Biophys. J*. **63**, 1165–1169 (1992).
[22] Radmacher, M., Tillmann, R. W., Fritz, M., and Gaub, H. E., *Science* **257**, 1900–1905 (1992).
[23] Akari, S. O., van der Vegte, E. M., Grim, P. C. M., Belder, G. F., Koutsos, V., ten Brinke, G., and Hadziioannou, G., *Appl. Phys. Lett*. **65**, 1915–1917 (1994).
[24] Overney, R. M., Meyer, E., Frommer, J., Guentherodt, H.-J., Fujihira, M., Takano, H., and Gotoh, Y., *Langmuir* **10**, 1281–1288 (1994).
[25] Radmacher, M., Fritz, M., Cleveland, J. P., Walters, D. A., and Hansma, P. K., *Langmuir* **10**, 3809–3814 (1994).
[26] Radmacher, M., Fritz, M., Hansma, H. G., and Hansma, P. K., *Biophys. J*. **69**, 264–270 (1995).
[27] Radmacher, M., Fritz, M., Kacher, C. M., Cleveland, J. P., and Hansma, P. K., *Biophys. J*. **70**, 556–567 (1996).
[28] Nie, H.-Y., Motomatsu, M., Mizutani, W., and Tokumoto, H., *Thin Solid Films* **273**, 143–148 (1996).
[29] Hansma, H. G., Kim, K. J., Laney, D. E., Garcia, R. A., Argaman, M., Allen, M. J., and Parsons, S. M., *J. Struct. Biol*. **119**, 99–108 (1997).
[30] Magonov, S. N. and Reneker, D. H. *Annu. Rev. Mater. Sci*. **27**, 175–222 (1997).
[31] Hofmann, U. G., Rotchs, C., Parak, W. J., and Radmacher, M., *J. Struct. Biol*. **119**, 84–91 (1997).
[32] Akhremitchev, B. B. and Walker, G. C., *Langmuir* **15**, 5630–5643 (1999).
[33] Sun, Y., Akhremitchev, B. B., and Walker, G. C., *Langmuir* **20**, 5837–5845 (2004).
[34] Singh, C., Pickett, G. T., Zhulina, E., and Balazs, A. C., *J. Phys. Chem. B* **101**, 10614–10624 (1997).
[35] Zhulina, E. B., Birshtein, T. M., Pryamitsyn, V. A., and Klushin, L. I., *Macromolecules* **28**, 8612–8620 (1995).

[36] Zuhulina, E., Walker, G. C., and Balazs, A. C., *Langmuir* **14**, 4615–4622 (1998); Fritz, J., Katopodis, A. G., Kolbinger, F., and Anselmetti, D., *Proc. Natl. Acad. Sci. USA* **95**, 12283–12288 (1998).
[37] Flory, P. J., *Statistical Mechanics of Chain Molecules* (Interscience Publishers, New York, 1969).
[38] Bemis, J., Akhremitchev, B. B., and Walker G. C., *Langmuir* **15**, 2799–2805 (1999).
[39] Ghatak, A., Vorvolakos, K., She, L., Malotky, D., and Chaudhury, M. K., *J. Phys. Chem. B* **104**, 4018–4030 (2000).
[40] Kavanagh, C. J., Swain, G. W., Kovach, B. S., Stein, J., Darkangelo-Wood, C., Truby, K., Holm, E., Montemarano, J., and Meyer, A., *Biofouling* **19**, 381–390 (2003).
[41] Callow, M. E., Callow, J. A., Ista, L. K., Coleman, S. E., Nolasco, A. C., and Lopez, G. P., *Appl. Env. Microbiol.* **66**, 3249–3254 (2000).
[42] Hu, H., Lingelser, J. P., and Gallot, Y., *Macromolecules* **28**, 5209–5214 (1995).
[43] Johnson, K. L., Kendall, K., and Roberts, A. D., *Proc. R. Soc. London, Ser. A* **324**, 301–313 (1971).
[44] Pedri, L., Itie, S., Schraft, H., and Hawton, M., "Bacterial Interaction with Hydrophobic and Hydrophilic Interfaces," Meeting Abstract, American Physical Society, 2004, Abstract number N9.015.
[45] Zhu, C., Bao, G., and Wang, N., *Ann. Rev. Biomed. Eng.* **2**, 189–226 (2000).